HOSTED BY

ELSEVIER

Available online at www.sciencedirect.com

ScienceDirect

journal homepage: http://ees.elsevier.com/ejbas/default.asp

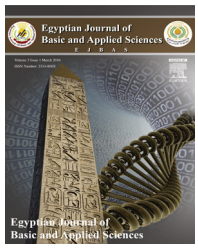

Full Length Article

Microstructural evolution and characterization of super-induced MgO composite on zinc-rich coatings

O.S.I. Fayomi [a,b,*], O.O. Joseph [a], M.P. Mubiayi [c], B.M. Durodola [d], O. Gabriel [a]

[a] Department of Mechanical Engineering, Materials and Corrosion Laboratory, Covenant University, P.M.B 1023, Ota, Ogun State, Nigeria

[b] Department of Chemical, Metallurgical and Materials Engineering, Tshwane University of Technology, P.M.B. X680, Pretoria, South Africa

[c] Department of Mechanical Engineering, University of Johannesburg, Kingsway Campus, P.O BOX 524, Johannesburg, South Africa

[d] Department of Chemistry, Covenant University, P.M.B 1023, Ota, Ogun State, Nigeria

ARTICLE INFO

Article history:
Received 28 January 2015
Received in revised form 17 May 2015
Accepted 29 May 2015
Available online 24 June 2015

Keywords:
Thermal performance
Zn-MgO
Ceramic film
Corrosion
Microstructure

ABSTRACT

The effect of Zn-MgO deposition prepared through direct electrolytic co-deposition on mild steel was studied. The experiment was conducted at current density between 0.5 and 1 A/cm^{-2}. The morphologies of the coated surfaces were characterized using Atomic Force Microscope (AFM), high resolution Nikon Optical Microscope (OPM) and Scanning Electron Microscopy attached with Energy Dispersive Spectrometer (SEM/EDX). The corrosion behavior was studied using linear potentiodynamic polarization method in 3.5% simulated environment. The phase change was evaluated using X-ray Diffractogram (XRD). The microhardness characteristics of the obtained deposits were analyzed with dura scan hardness tester. The stability of the ceramic composite was determined using heat-treatment processes at 200 °C for 4 h. The results show that the structural behavior and corrosion resistance of the coating is dependent on the composite induced particulate and applied current density. It is found that increasing MgO contents beyond optimum level does not cause increase in microhardness progression. A decrease in applied current maximally influences the deposit adhesion characteristics. The enhanced thermal stability of 236.4 HVN for Zn-20MgO at 0.5 A/cm^2 alloy and increase corrosion behavior was thus attributed to its chemical composition, phase content and the synergistic effect of Zn and MgO on the carbon steel.

* *Corresponding author.* Tel.: +27719811277.
E-mail address: ojosundayfayomi3@gmail.com; ojo.fayomi@covenantuniversity.edu.ng (O.S.I. Fayomi).

http://dx.doi.org/10.1016/j.ejbas.2015.05.007

Table 1 – Chemical composition of mild steel used (wt %).

Element	C	Mn	Si	P	S	Al	Ni	Fe
Composition	0.15	0.45	0.18	0.01	0.031	0.005	0.008	Balance

1. Introduction

Co-deposition with the help of composite coating is a straightforward and cost-effective method of preventing corrosion and mechanical failure. The presence of certain alloying elements in the bath considerably affects the morphology, growth and kinetics of coating. However, with the choice of proper plating parameters, electrodeposition can still give better coatings with fine surface finish that will exhibit high degree of corrosion resistance and mechanical properties such as micro-hardness, wear resistance, ductility, strength and decorative properties [1–6]. Research has shown that the characteristics of deposited coatings depend on several factors which include pH, current density, applied voltage, bath composition temperature and additives [6–16].

The use of Zn metal for composite coatings is finding increased interest in surface technology and corrosion protection, owing to its superior corrosion and wear resistance in addition to extended lifetime. However, the use of Zn matrix in the generation of composite coatings is scanty compared to Cu, Ni and other alloys [17–20]. Thin films of Ti-Si-N by physical vapor deposition (PVD) were prepared with the intention to improve the wear resistance of TiN coatings [18–23]. The influence of Zn-TiO_2 deposits on the surface morphology of a metal was studied [14–19] and it was concluded that the nanoparticles have a strong influence on the deposit surface morphology. Several studies [24–29] among others have revealed that the corrosion resistant properties of Zn coatings can be significantly improved upon by alloying with other transition metals and oxides such as Ni, Co, Cr, Sn, and TiO. In contrast to these alloying metals, information about the effect of varying additions of MgO to Zn coatings is sparse in the literature. In the present study, effects of the bath composition and deposition potentials on the physical and electrochemical properties of Zn-MgO coatings are discussed. Corrosion protection properties were analyzed using linear polarization, Tafel analysis and corrosion rate in 3.65% sodium chloride solution at 40 °C.

The aim of this work is to investigate the influence of MgO in zinc rich concentrations with consideration of their structural, corrosion resistance properties, hardness and thermal studies.

2. Materials and methods

2.1. *Electrodeposition process*

The formulated deposition bath was composed of 150 gL^{-1} ZnCl, 70 gL^{-1} KCl, 20–40 gL^{-1} MgO, 10 gL^{-1} H_3BO_3, 5 gL^{-1}glycine, and 5 gL^{-1} thiourea. Analytical reagents and deionized water were used to prepare the plating solution. Before co-deposition, the MgO particulates of 20 ηm were incorporated into the bath electrolyte in the presence of other additives. The deposition setup tests were achieved on a setup vessel connected to a laboratory rectifier. The bath was stirred by a magnetic stirrer consistently with about 100 rpm at 40 °C. The experiments were conducted at current density between 0.5 and 1 Acm^{-2} and applied potential of 0.3–0.6 volts. A carbon steel sheet of 20 mm × 40 mm × 2 mm was used as the cathode. A sectioned rectangular zinc plate of a size 25 mm × 50 mm × 3 mm with a well prepared surface was used as the cathode substrate to be plated. The chemical composition of the substrate is described in Table 1 and the varied deposited parameters are illustrated in Table 2.

Prior to deposition, the working substrates were polished mechanically, degreased and rinsed with water. The surface preparation was carried out using a polishing machine with emery papers in the order of 60 μm, 120 μm, 400 μm, 800 μm and 1600 μm grades. The substrates were sequentially cleaned in ethanol and distilled water for 10 minutes, rinsed with 5 % H_2SO_4, washed in distilled water, and then dipped instantaneously in the bath formulated to allow the deposition of the target ceramic composite coatings.

2.2. *Microhardness measurement*

The microhardness along the surface of the coated sample was measured with a high Dura Diamond based Vickers' microhardness tester. An indention load of 50 g and loading time of 10 s were used in this study. The average equal distance of indent was made and average mean value was obtained.

Table 2 – Experimental study parameter of Zn-MgO ceramic composite deposition.

Sample order	Material sample	Time of deposition (min)	Current density(A/cm^2)	Concentration of additive (g)
Blank	–	–	–	–
Sample 1-B1	Zn-20-MgO	15	0.5	20
Sample 2-B2	Zn-20MgO	15	1.0	20
Sample 3-B3	Zn-40MgO	15	0.5	40
Sample 4-B4	Zn-40MgO	15	1.0	40

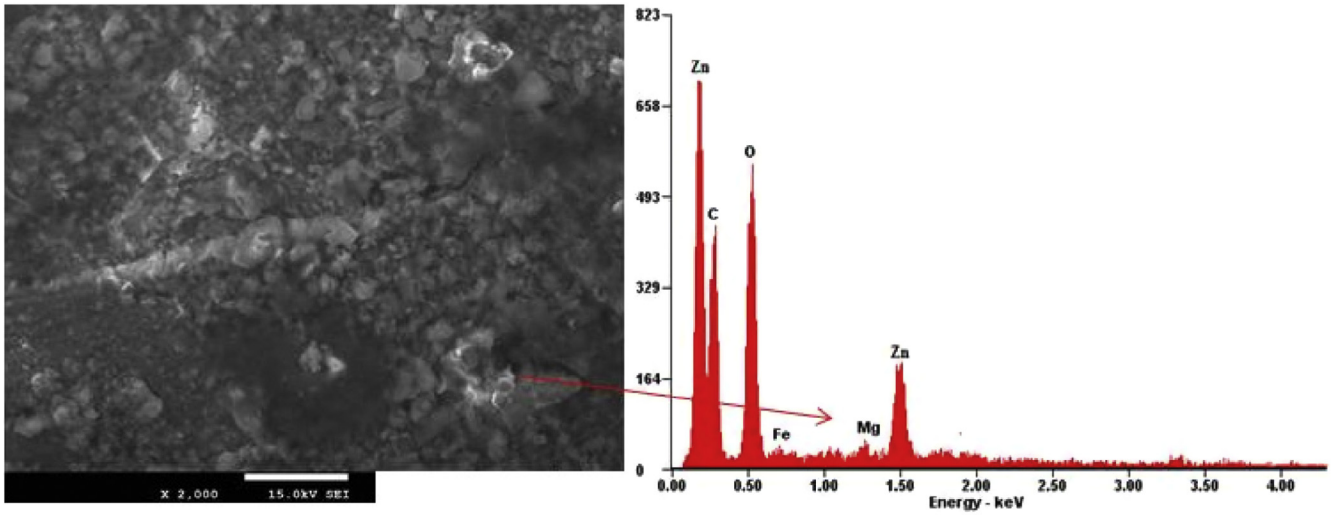

Fig. 1 – Micrograph of Zn-20MgO-0.5 A/cm² deposited on mild steel.

2.3. *Structural and phase composition*

Chemical composition of the Zn/MgO MMC coatings produced by the electrolytic deposition method was investigated using the scanning electron microscope(SEM) equipped with energy dispersive X-ray spectrometer (EDS). Phase identification was carried out with a PANalytical EMPYREAN X-ray diffractometer using the CuKα radiation and operating at 45 kVand40mA and 25 °C.

2.4. *Electrochemical study*

The electrochemical studies were performed with Auto lab PGSTAT 101 Metrohm Potentiostat using a three-electrode cell assembly in a 3.65% NaCl static solution at 40 °C. The developed composite was the working electrode, platinum electrode was used as the counter electrode and Ag/AgCl was used as the reference electrode. The anodic and cathodic polarization curves were recorded by a constant scan rate of 0.012 V/s which was fixed between ±1.5 mV. From the Tafel corrosion analysis, the corrosion rate, potential and linear polarization resistance was obtained.

3. Results and discussion

3.1. *Morphological characterization*

Microstructures of the composite coating produced by Zn-MgO alloy are shown in Figs. 1 and 2. The structural image of Zn/MgO deposited alloy at additive concentration of 20 g in 0.5 A/cm² produced a homogenous, smooth and more stable modification with Mg disperses along the interface. In this case the coatings were well bonded to the substrate and the EDX indicate major element admixed constituent expected. It should be noted that the overall content of MgO is much stable due to the moderate nucleation progression and rate of transfer of the particulates in relation to the optimum process

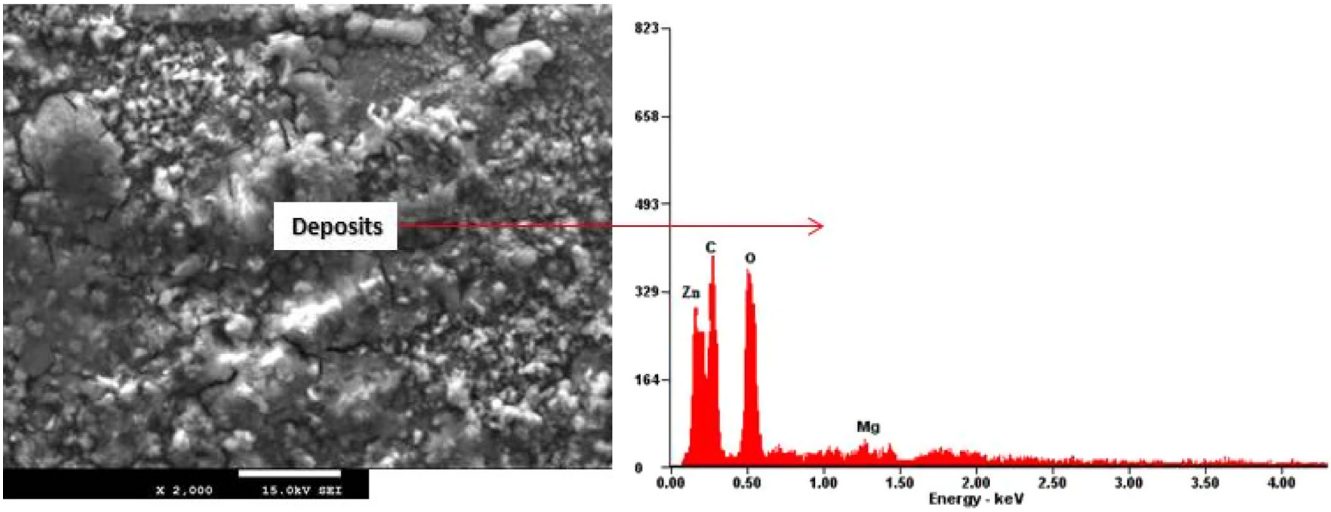

Fig. 2 – Micrograph of Zn-40MgO-1.0 A/cm² deposited on mild steel.

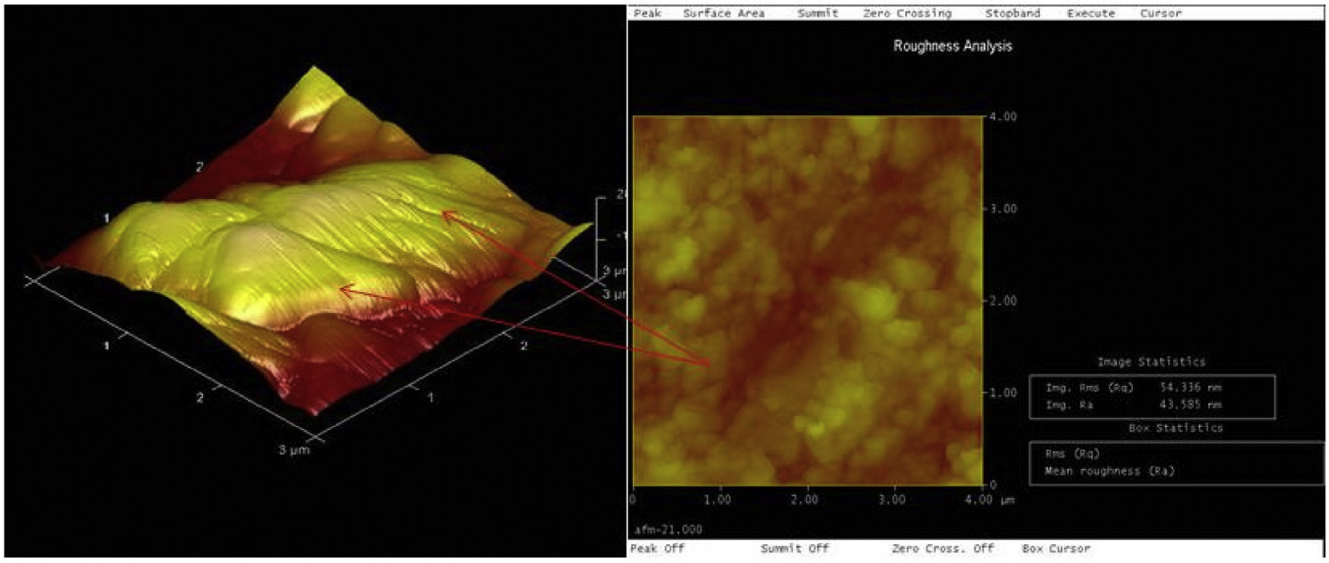

Fig. 3 – AFM topographic pattern of Zn-20MgO-0.5A/cm$^{2.}$

variable. This observation is in accordance with the reported case [17–19] that with proper process parameter and optimum composite incorporation range, spherical crystallites with dendrites free structure often occur which notably give rise to solid adhered coatings.

On the other hand, the microstructure of the coating produced by Zn-40MgO at 1.0 A/cm^2 was characterized with agglomeration of the solid crystal with few dispersed film which refuse to adhere properly. This challenge is associated with an increase in the particulate in the bath electrolyte which significantly affects the rate of transfer of films from the anodic region. In other words, the characteristic feature of this coating was micro-segregation in nature due to excessive doping of the ceramic oxide in the zinc rich electrolyte.

Addition of MgO was found not to support and contribute to the enrichment of the metal matrix coating as expected due to diffusion problem. However, a reported study [21] pointed out that adhesion behavior of a coating doesn't necessarily depend on the fraction volume but the degree of dissolution assisted by the process control parameter at optimum range.

In order to have deep perception of the surface morphology of the deposited films, the atomic force microscopy was used to characterize the topographical pattern of Zn-20MgO-0.5 A/cm^2 as indicated in Fig. 3. A spherical crystalline showing

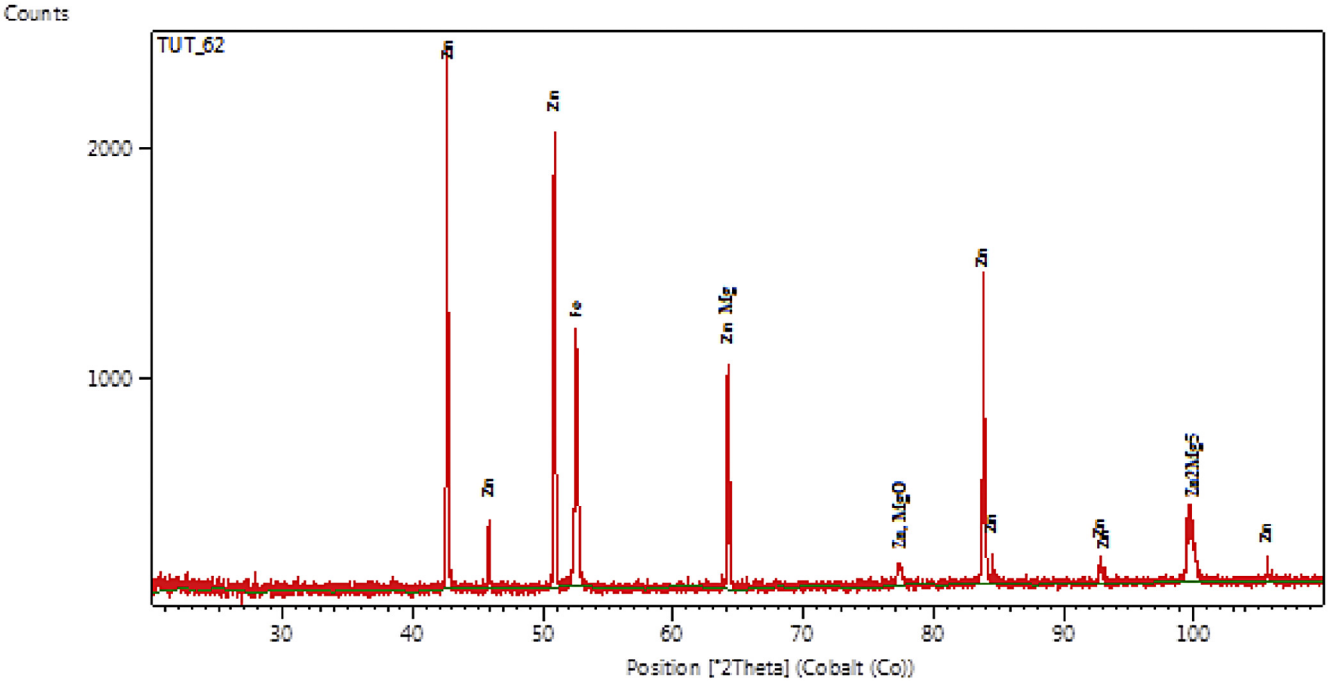

Fig. 4 – XRD phase pattern of Zn-20MgO-0.5A/cm^2 deposited on mild steel.

visible preciptate with distinctive topography of the embedded particulate was observed.

Results from XRD patterns of specimens obtained for Zn-20MgO-0.5 A/cm^2 is shown in Fig. 4. The produced coating shows high intensity phases containing intermetallic intermediate of Zn, ZnMgO, Zn_2Mg_5, and ZnMg. The results were consistent with the EDSX-ray microanalysis. The main peaks found are with Zn, at 2θ *Braga angle intensity of* = 38.12°, 52.10° and 84.22°. From observation, new phase orientation of the metal particles precipitate for Zn/Mg admixed at 64.52°, 78.11° and 100.10°. With these formed phases, a complete dissolution of the participated composite was noted on zinc rich content, although enhanced buildup of strong intermetallic precipitates gives rise to the fine grain microstructures observed.

Fig. 5a–d shows the thermo-structural behavior of heat treatment produced coating at 200 °C for 4 h. The produced coating at Zn-20MgO-0.5 A/cm^2 (Fig. 5a) shows good resilience to thermal deformation although with few affected heat zones observed within the interface compared to other coatings with severe heat treated pit. Figs. 5b,c follow the same trend as the former but with more heat infringement within the lattice. The Zn-40MgO-1.0 A/cm^2 coating in Fig. 5d shows a massive distortion of the grains crystal due to the initial agglomeration and poor adhesion characteristics. It is however necessary to mention that the recrystallization tendency often depends on the process parameter [22,24] and this could outrightly influence the resilient behavior of deformation propagation. Thermal treatment resulted in evolution of MgO and pinholes were observed at 1.0 A/cm^2. Nevertheless, the most improved surface characteristic after thermal treatment was obtained with Zn-20MgO deposition at current densities of 0.5 A/cm^2.

3.2. *Microhardness studies*

The average microhardness values of the deposited coatings are shown in Fig. 6 with correlation of individual matrices. From

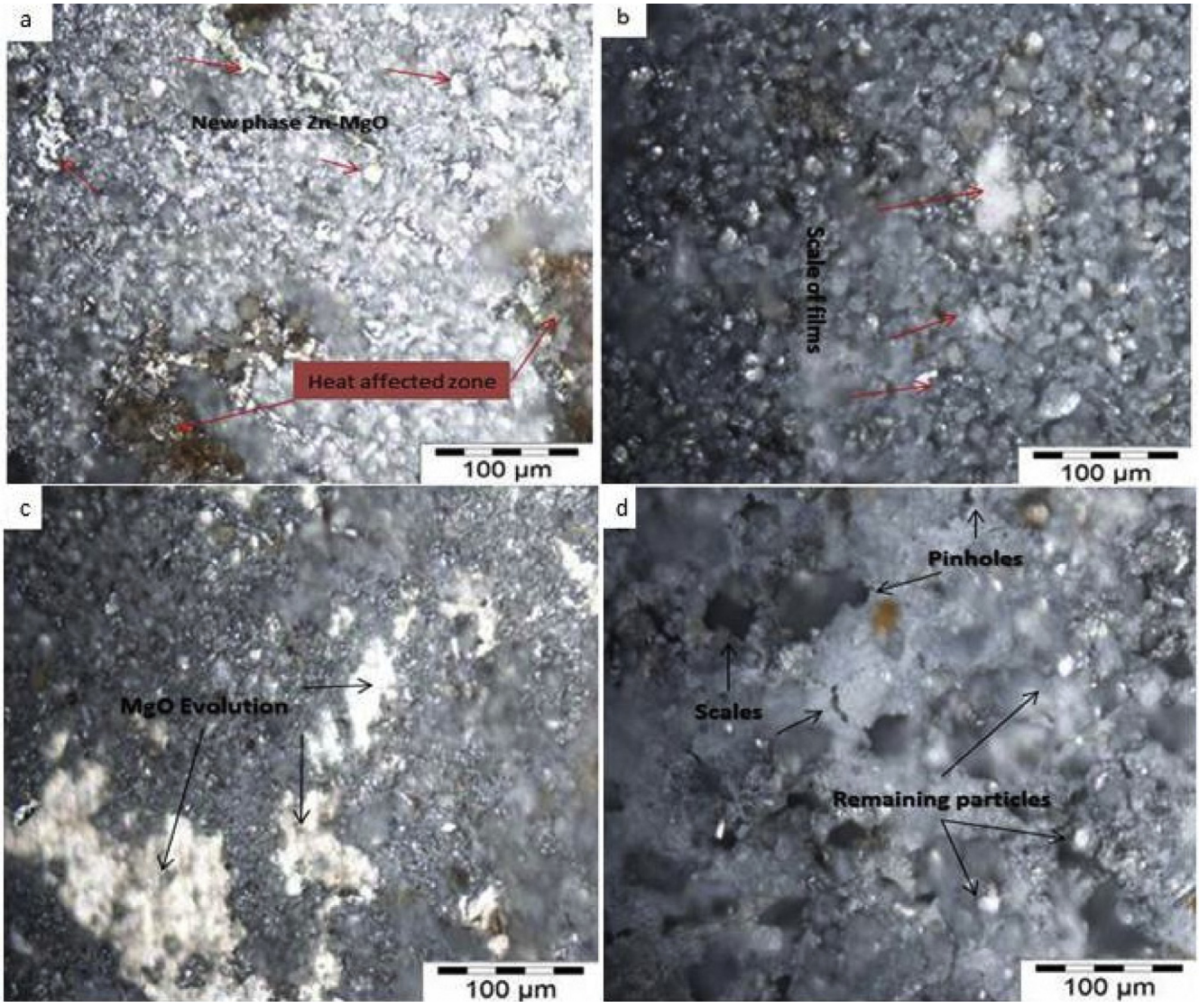

Fig. 5 – Micrograph of (a) Zn-20MgO-0.5 A/cm^2, (b) Zn-20MgO-1.0 A/cm^2, (c) Zn-40MgO-0.5 A/cm^2, and (d) Zn-40MgO-1.0 A/cm^2.

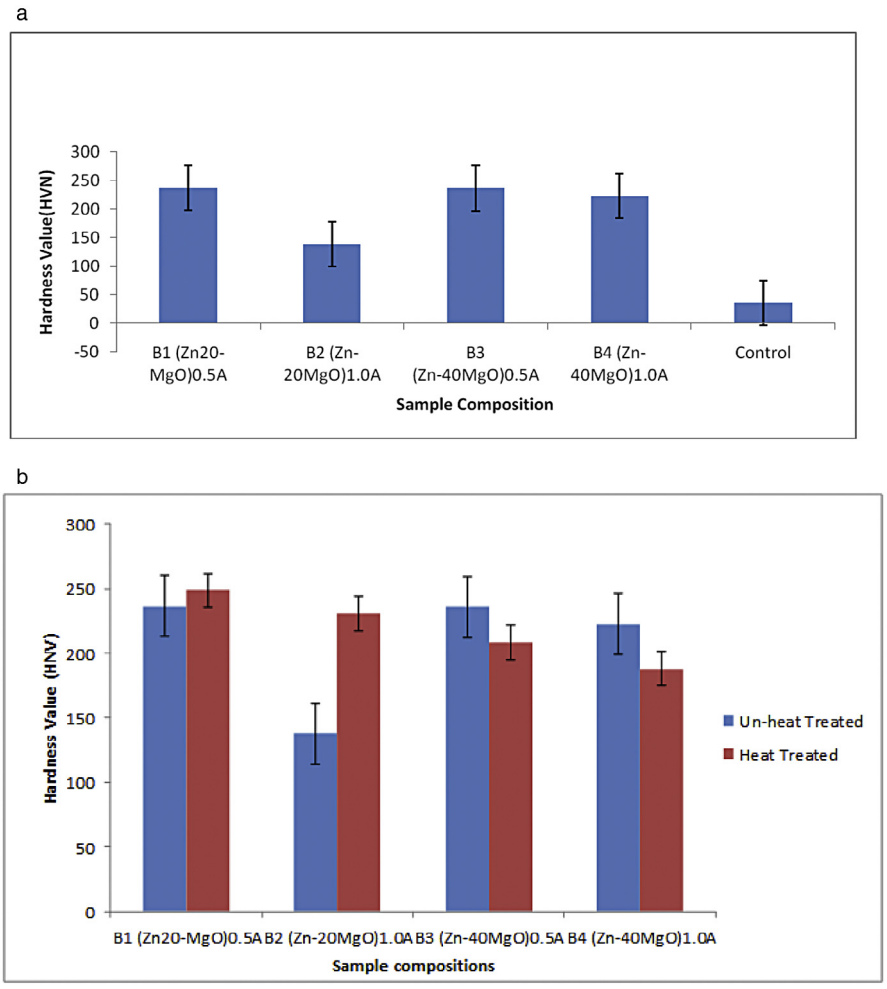

Fig. 6 – (a) The microhardness/depth profile for Zn-MgO deposited sample. (b) The Hardness of the samples deposited on mild steel before and after thermal treatment.

the hardness trend, the control sample had a hardness value of 35 HVN. The hardness profile data for all the deposited coating show significant increase with 137.94 HVN for Zn-20MgO at 1.0 A/cm^2, followed by 222.6 HVN for Zn-40MgO at 1.0 A/cm^2. The most improved hardness property was 236.4 HVN by Zn-20MgO at 0.5 A/cm^2. From all facts, the improvements in hardness obviously provide a geometric increase over the substrate and this was attributed to the crystal formation and superior nucleation. The adhesion and nucleation which yield the significant microhardness are reported to depend on the operating condition. Previous works [13,14,22] had affirmed that the microstructure evolved in coating is linked to processing parameters and hence provide grain size which is paramount to the buildup of surface hardness as shown by our result.

Upon observation and comparison of the surface hardness of the depositions before and after thermal treatment as shown in Fig. 6b, only Zn-20-MgO exhibited increased hardness at both 0.5 A/cm^2 and 1.0 A/cm^2. For Zn-40-MgO, there was decreased hardness after thermal treatment for other alloy matrices. The reason for this non-improved property after thermal response might be because of the severe pile up due to unstable adhesion of the coating film which was obtained from Zn-20-MgO in 0.5 A/cm^2.

3.3. *Electrochemical test result of deposited alloys*

Fig. 7 shows the progression of deterioration and the susceptibility to corrosion in 3.65% simulated medium with an induced current propagation examined using potential/current measurements. Linear potentiodynamic polarization data for coated and control samples are shown in Table 3. The differences in the potential values of the deposition were considered at 10 MA applied current. In all cases of the coated samples, the potential values increased as compared with the corrosion potential of the control sample (–1.53900 V). More so, the corrosion rate and current density decreased considerably for all coated alloy matrix. This is an indication that the deposited coatings produced an excellent bonding and adhesion with the substrate material. Furthermore, the coatings have a strong resistance to corrosion which is reflected in the decreased corrosion rate. Even though the behavior of the as-received sample is expected [21], it is also important to mention that the degree of ceramics composite incorporation in little quantity has a

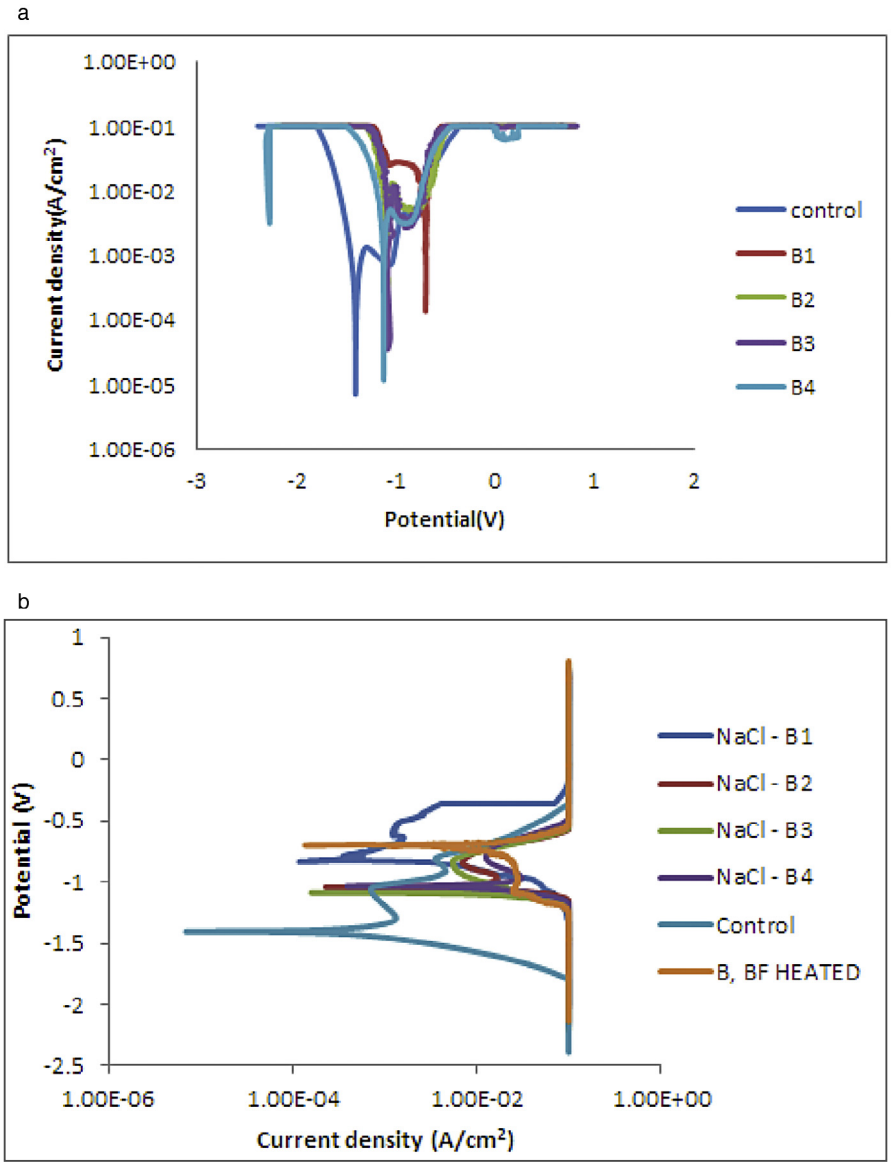

Fig. 7 – (a) The Linear Polarization plot of current density for corrosion against the potential. (b) Electrochemical polarization study of deposited alloys after heat treatment.

proven capacity to provide solid resistance against chloride attack.

3.4. *Thermo-chemical properties*

Fig. 7b and Table 3b present corrosion resistance behavior of the coated and uncoated samples after thermal treatment. From observation, all thermally treated coating matrices show slight decrease in corrosion rate and current density as compared to unthermally treated coatings. In fact, the corrosion potential in all cases decreased after thermal treatment. It can be said that thermal treatment of the deposited binary coatings does not really improve the corrosion resistance but rather verify the degree of stability obtained in harsh environment. In view of this, the corrosion resistance of the coated samples increased in the following order: B1 > B4>B2 > B3 and Control. With the Rp values of 27.600 (Ω), B1 (Zn-20MgO) 0.5 A/cm^2 coating still maintained its passive characteristic cession rate of 0.2241 mm/yr compared to the as-received sample with 4.1 mm/yr. The unthermally treated alloy possesses a significant reduction in all with a corrosion rate of 4.1 mm/yr. Invariably, it can be deduced that the rate of deformation are dependent on the degree of protection and the induced condition the component produced.

The optical micrograph of the thermally heat treated alloy matrices were presented in Figs. 8 and 9 to examine the deformation progression from both thermal-chemical induced environment. From all indication, Zn-20MgO-0.5 A/cm^2 and Zn-20MgO-1.0 A/cm^2 coatings show the presence of initiated oxide films at the interface. The even dispersion of the crystals was not well noticed due to the impact of thermo-corrosion strain induced. For Zn-40MgO-0.5A/cm^2 and Zn-40MgO-1.0 A/cm^2

Table 3 – (a) Linear potentiodynamic polarization data for coated and uncoated samples in 3.65% NaCl solution. (b) Linear potentiodynamic polarization data for coated and uncoated heat treated samples in 3.65% NaCl solution.

a

Sample	E_{corr}, Obs (V)	j_{corr} (A/cm^2)	C_r (mm/yr)	R_p (Ω)
B1(Zn-20MgO)0.5A	–0.7085	2.94E-03	2.1442	109.04
B2(Zn-20MgO)1.0A	–1.0972	3.54E-03	2.6320	37.343
B3(Zn-40MgO)0.5A	–1.0723	3.79E-03	2.3891	44.325
B4(Zn-40MgO)1.0A	–1.0880	5.55E-03	2.6320	42.213
Control	–1.5390	7.04E-02	41	27

b

Sample	E_{corr}, Obs (V)	j_{corr} (A/cm^2)	C_r (mm/yr)	R_p (Ω)
B1 HT	–0.8483	3.69E-03	0.2241	38.847
B2 HT	–1.0365	4.65E-03	0.2864	37.691
B3 HT	–1.0880	8.11E-03	0.2155	29.318
B4 HT	–1.0219	3.40E-03	0.7760	32.308
Control	–1.5390	7.04E-02	41	27.600
B1(Zn-20MgO)0.5A	–0.7085	2.94E-03	2.1442	109.04

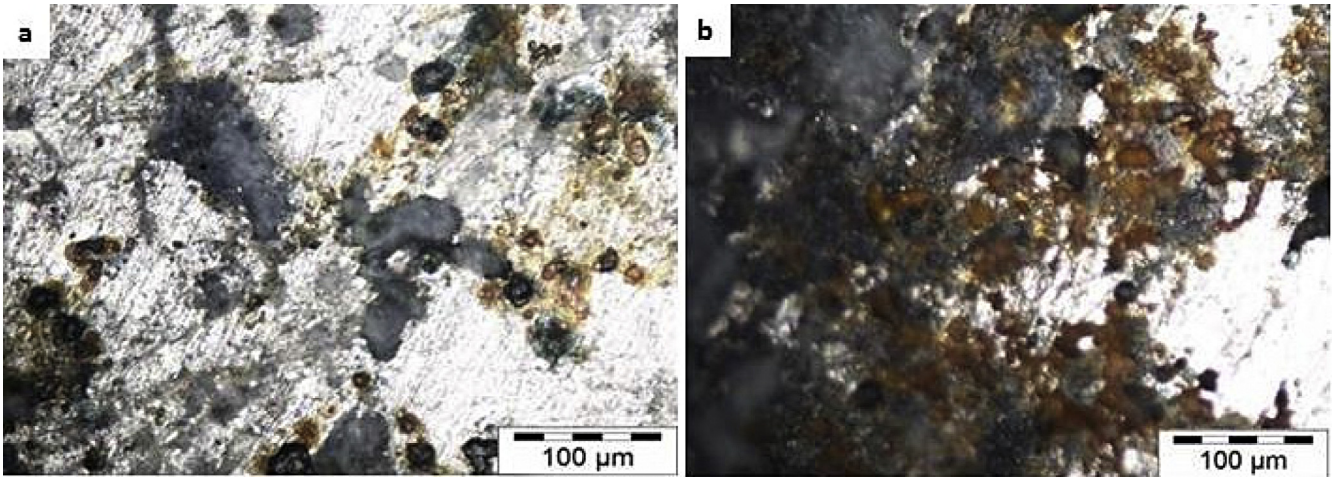

Fig. 8 – Micrograph of corrosion studies of (a) Zn-20MgO-0.5 A/cm^2 and (b) Zn-20MgO-1.0 A/cm^2 deposited after thermal treatment.

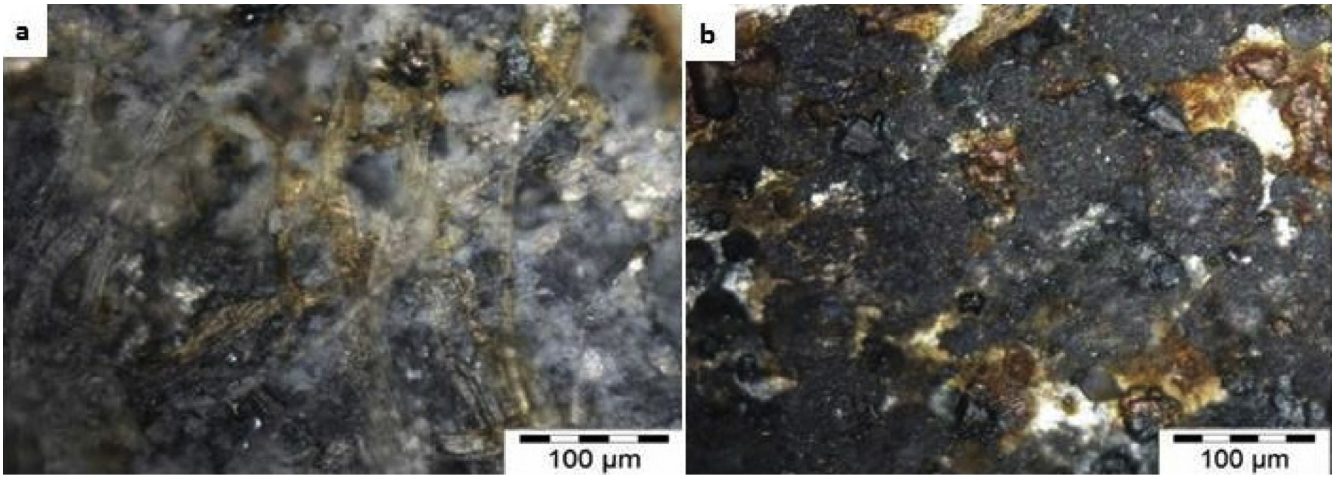

Fig. 9 – Micrograph of corrosion studies of (a) Zn-40MgO-0.5 A/cm^2 and (b) Zn-40MgO-1.0 A/cm^2 deposited after thermal treatment.

(Fig. 9) coatings, there are visible appearances of corrosion products at the interfaces due to penetration of thermal-oxidation activities. Obviously the presence of ions of Zn^{2+} and Mg^{2+} could not resist sufficiently the induced activity as expected but rather aggravated the dissolution and corrosion product seen all over the interface.

4. Conclusion

The microstructure, thermal-oxidation and micro-mechanical properties of Zn-MgO induced composite coatings have been studied. From the results, the deposition of admixed binary composite particles in the presence of the MgO ceramic particulate significantly enhanced both mechanical and corrosion performance of the coatings. The most improved hardness property was 236.4 HVN by Zn-20MgO at 0.5pA/cm^2. New crystalline structures are formed as a result of heat-treatment, with Zn-20MgO at 0.5pA/cm^2 coatings still maintaining its performance, thereby possessing best properties among all series. Thermal stability of the composite coating improved with moderate addition of MgO into the Zn^{2+} interface. Good morphology significantly distorts easy penetration of the temperature that engenders stability of the coated alloy.

Acknowledgement

The authors deeply appreciate the research effort made by Covenant University and Tshwane University of Technology to bring this work to a reasonable conclusion. Laboratory input of Surface Engineering Research Center (SERC) is also recognized.

REFERENCES

[1] Praveen BM, Venkatesha TV. Appl Surf Sci 2008;254:2418–24.
[2] Chuen-Chang L, Chi-Ming H. J Coat Technol Res 2006;3:99–104.
[3] Mohankumar C, Praveen K, Venkatesha V, Vathsala K, Nayana O. J Coat Technol Res 2012;9:71–7.
[4] Arici M, Nazir H, Aksu A. J Alloys Comp 2011;509:1534–7.
[5] Popoola API, Fayomi OS. Int J Electrochem Sci 2011;6:3254.
[6] Yang G, Chai S, Xiong X, Zhang S, Yu L, Zhang P. Trans Nonferrous Met Soc China 2012;22:366–72.
[7] Xu R, Wang J, Guo Z, Wang H. J Rare Earth 2008;26:579–83.
[8] Fayomi OSI, Popoola API. Res Chem Intermed 2013;39:6. doi:10.1007/s11164-013-1354-2.
[9] Popoola API, Fayomi OSI, Popoola OM. Int J Electrochem Sci 2012;7:4898–917.
[10] Shibli SMA, Chacko F, Divya C. J Corros Sci 2010;52:518–25.
[11] Abdel AA, Hassan HB, Rahim MA. J Electroanal Chem 2008;620:17–25.
[12] Fayomi OSI, Abdulwahab M, Popoola API. J Ovionic Res 2013;9:123–32.
[13] Abdel A, Barakat MA, Mohammed RM. Appl Surf Sci 2008;254:4577–83.
[14] Fustes J, Gomes A, Da Silva Pereira MI. J Solid State Electrochem 2008;12:1435–43. doi:10.1007/s10008-007-0485-z.
[15] Popoola API, Fayomi OSI, Popoola OM. Int J Electrochem Sci 2012;7:4860–70.
[16] Rahman MJ, Sen SR, Moniruzzaman M, Shorowordi KM. J Mech Eng 2009;40:9–12.
[17] Fayomi OSI, Popoola API, Loto CA. Int J Electrochem Sci 2014;9:3885–903.
[18] Fayomi OSI, Popoola API, Inegbenebor AO. Multiple loading and mechanical response of Al6O13Si2–ZrO2/Zn composite coating. Results Phys 2014;4:79–80.
[19] Fayomi OSI, Popoola API. Egypt J Basic Appl Sci 2014;4:1–6.
[20] Fayomi OSI, Popoola API, Loto CA. J Compos Mater 2014;9:1–13. doi:10.1177/0021998314552002.
[21] Fayomi OSI, Popoola API. J Alloys Comp 2014;617:455–63.
[22] Vathsala K, Venkatesha T V. Appl Surf Sci 2011;257:8929–36.
[23] Diserens M, Patscheider J, Levy F. Surf Coat Tech 1998;108–109:241–6.
[24] Sancakoglu O, Culha O, Toparli M, Agaday B, Celik E. Mater Des 2011;32:4054–61.
[25] Lehmberg CE, Lewis DB, Marshall GW. Surf Coat Tech 2005;192:269–77.
[26] Ranganatha S, Venkatesha TV, Vathsala K, Punith Kumar MK. Surf Coat Tech 2012;208:64–72.
[27] Fayomi OSI, Popoola API, Aigbodion VS. J Alloys Comp 2014;623:328–34.
[28] Fayomi OS I, Loto CA, Popoola API, Tau V. Int J Electrochem Sci 2014;9:7359–68.
[29] Fayomi OSI, Aigbodion VS, Popoola API. J Fail Anal Prev 2014;doi:10.1007/s11668-014-9908-1.